frontiers | Frontiers in Marine Science

TYPE Original Research
PUBLISHED 25 September 2024
DOI 10.3389/fmars.2024.1464095

OPEN ACCESS

EDITED BY
Elva G. Escobar-Briones,
National Autonomous University of Mexico, Mexico

REVIEWED BY
Marina R. Cunha,
University of Aveiro, Portugal
Aldo S. Pacheco,
Royal Roads University, Canada

*CORRESPONDENCE
Fabio C. De Leo
fdeleo@uvic.ca

RECEIVED 13 July 2024
ACCEPTED 26 August 2024
PUBLISHED 25 September 2024

CITATION
Smith CR, Correa PVF, Fleury AG, Levin LA and De Leo FC (2024) High-frequency study of megafaunal communities on whale bone, wood and carbonate in hypoxic Barkley Canyon.
Front. Mar. Sci. 11:1464095.
doi: 10.3389/fmars.2024.1464095

High-frequency study of megafaunal communities on whale bone, wood and carbonate in hypoxic Barkley Canyon

Craig R. Smith[1,2], Paulo V. F. Correa[2], Aharon G. Fleury[3,4], Lisa A. Levin[5] and Fabio C. De Leo[2,3]*

[1]School of Ocean Earth Science and Technology, University of Hawaii at Manoa, Honolulu, HI, United States, [2]Ocean Networks Canada, University of Victoria, Victoria, BC, Canada, [3]Department of Biology, University of Victoria, Victoria, BC, Canada, [4]Centre for Biodiversity and Conservation Science, The University of Queensland, Brisbane, QLD, Australia, [5]Center for Marine Biodiversity and Conservation and Integrative Oceanography Division, Scripps Institution of Oceanography, UC San Diego, La Jolla, CA, United States

Organic-rich whale bones and wood falls occur widely in the deep sea and support diverse faunal communities, contributing to seafloor habitat diversity. Changes in community structure through succession on deep-sea bone/wood substrates are modulated by ecosystem engineers, i.e., bone-eating *Osedax* annelids, and wood-boring *Xylophaga* bivalves. Here, we use a comparative experimental approach and Ocean Networks Canada's (ONC) cabled observatory in hypoxic Barkley Canyon to study, at high temporal resolution, colonization and succession on whale-bone, Douglas fir wood, and control carbonate rock over 8.3 mo. Experimental substrates were similar in size and mounted on PVC plates near the seafloor at 890 m depth and monitored by high-definition video camera for 5-min intervals every 6-12 h over a period of 8.3 mo. A broad range of seafloor and sea-surface environmental variables were also monitored at this site over the 8.3 mo to account for environmental variability and food input. Following loss of the high-definition camera, substrates were surveyed approximately annually with lower resolution ROV video for an additional 8.5 y. We find that megafaunal abundances, species diversity, and community structure varied substantially over 8.3 mo on each substrate, with markedly different patterns on whale bones due to the development of extensive white bacterial mats. A combination of seafloor and sea surface variables explained < 35% of bone/wood community variation. Bone-eating *Osedax* annelids failed to colonize whale bones even after 9.2 years, and boring *Xylophaga* bivalves colonized the wood at much lower rates than in better oxygenated deep-sea locations. Species diversity on whale-bone and wood substrates appeared to be substantially reduced due to the absence of ecosystem engineers and the low oxygen concentrations. We hypothesize that *Osedax/Xylophaga* colonization, bone/wood degradation, and bone/wood

community development may be limited by oxygen concentrations of 0.22 - 0.33 ml.l on the NE Pacific margin, and that OMZ expansion due to climate change will reduce whale-bone and wood degradation, and the contribution of whale falls and wood falls to beta diversity, on the NE Pacific margin.

KEYWORDS

deep sea, organic falls, whale bone, wood, cabled observatory, oxygen minimum zone, NE Pacific, time-lapse video

1 Introduction

Organic-rich habitat islands support specialized micro-communities throughout natural ecosystems and often play fundamental roles in maintaining alpha and beta diversity by facilitating adaptive radiation and evolutionary novelty (Smith et al., 2015). Non-marine examples include tree falls in forest ecosystems, ungulate dung piles in fields and savannahs, mammalian carcasses in tropical to polar habitats, as well as leaflitter, carcass and wood accumulations in forests and streams (e.g., Schoenly and Reid, 1987; Schaetzl et al., 1989; Hanski and Cambefort, 1991; Hanski and Gilpin, 1997; Ulanova, 2000; Quaggiotto et al., 2019). Each of these habitat types harbors a characteristic biota distributed in metacommunities in which connectivity, adaptation and coevolution shape decomposer, trophic, and successional interactions, in turn influencing patterns of taxonomic, genetic, and functional diversity over a broad range of scales (Smith et al., 2015). Such organic-rich habitat islands have provided model systems for exploring processes of ecosystem function, community succession, biodiversity maintenance, metapopulation dynamics, and evolution in terrestrial and freshwater ecosystems (e.g., Hanski and Gilpin, 1997; Gessner et al., 2010; Smith et al., 2019).

Organic-rich habitat islands in the form of whale bones and wood falls also occur widely in the deep sea. These bone/wood islands can support diverse, trophically complex macro- to megafaunal communities and have sustained radiations of decomposer taxa (*Osedax* annelids and *Xylophaga* bivalves, respectively) adapted to exploit the concentrated organic matter trapped within a recalcitrant bone/wood matrix (e.g., Turner, 1973, 1977, 2002; Pailleret et al., 2007; Voight, 2008, 2009; Richer de Forges et al., 2009; Smith et al., 2015; Sumida et al., 2016; Alfaro-Lucas et al., 2017; Harbour et al., 2021a, 2021b; Young et al., 2022). For example, single deep-sea whale skeletons can support >200 species, and at least 129 newly described and putative new species from seven phyla have been collected on whale remains since 1987; this includes 31 described or putative species of bone-boring *Osedax* worms (Smith et al., 2015). Similarly, deep-sea wood falls support speciose faunal communities, including wood-boring decomposers (45 species of bivalves in the genus *Xylophaga*), and a substantial number of specialists utilizing wood falls for nutrition and habitat (Turner, 1973, 1977; Wolff, 1979; Distel and Roberts, 1997; Distel et al., 2000; Stoeckle, 2006; Pailleret et al., 2007; Voight, 2007, 2009; Gros et al., 2007; Bernardino et al., 2010; Rodriguez and Daly, 2010; Bienhold et al., 2013; Young et al., 2022). The communities on whale bones and wood falls are heavily influenced by ecosystem-engineering activities of substrate decomposers, i.e., *Osedax* and *Xylophaga*, that burrow into bone/wood, transform inaccessible organic material into biomass and/or labile fecal material, and create three-dimensional habitat structure in an initially solid substrate, thus modulating food and habitat availability for associated communities (Turner, 1973, 1977; Wolff, 1979; Stoeckle, 2006; Voight, 2007, 2008; Smith and Baco, 2003; Bienhold et al., 2013; Smith et al., 2015; Alfaro-Lucas et al., 2017; Young et al., 2022). Modification of the bone/wood substrates is caused by colonization and population growth of ecosystems engineers, as well other habitat-altering biota such as microbial mats, yielding successional changes on these organic-rich substrates (Smith and Baco, 2003; Bienhold et al., 2013; Smith et al., 2015; Young et al., 2022).

Fresh whale remains in the deep sea have been shown to pass through a series of successional stages including a mobile-scavenger stage in which soft tissue is consumed by carrion feeders such as lysianassid amphipods, hagfish and sleeper sharks, an enrichment opportunist stage supporting generalized and specialized heterotrophic species (e.g., capitellid polychaetes and *Osedax* worms, respectively) directly consuming labile whale organic material on/in bones and sediments (Smith et al., 2015; Alfaro-Lucas et al., 2017), and a sulfophilic stage in which anaerobic microbial degradation of bone lipids yields sulfides to support chemoautotrophic bacteria in microbial mats and within animal tissues (Smith et al., 2015; Alfaro-Lucas et al., 2017). Deep-sea wood falls also are thought to undergo community succession but lack a mobile scavenger stage; succession is thought to include a specialist stage where *Xylophaga* bivalves bore into the wood, an opportunist stage in which a diversity of predators and detritivores feed on the tissue and feces of the boring bivalves, a sulphophilic stage in which anaerobic decomposition of wood and bivalve feces supports chemoautotrophic communities, and finally a senescence stage characterized by die-out of *Xylophaga* and possibly disintegration of the wood (Bienhold et al., 2013; Pop Ristova et al., 2017; Young et al., 2022).

Nearly all successional changes on whale bones and wood falls have been documented by coarse-resolution time series, with typical intervals between observations of a few months to years (Smith and Baco, 2003; Lundsten et al., 2010a; Bienhold et al., 2013; Smith et al., 2015). Furthermore, studies of whale-bone and wood-fall succession have occurred in different deep-sea localities with very limited collection of environmental data (but see Young et al., 2022); this makes it difficult to compare rates and patterns of succession between substrate types, and to explore how changes in environmental conditions may influence community structure and succession over a broad range of time scales (hours to many months). Temporal variations are particularly important to assess because high-resolution studies of other energy-rich deep-sea habitats, including hydrothermal vents, methane seeps and submarine canyons, have revealed changes in benthic community structure and behavior in response to variations in bottom currents, oxygen concentration, temperature, and phytodetritus flux and seepage (e.g., Lelievre et al., 2017; Chauvet et al., 2018; Thomsen et al., 2017; Aguzzi et al., 2012, 2018; Chu et al., 2018; Pereira et al., 2021).

Here, we use a comparative experimental approach (c.f., Menge et al., 2002; Young et al., 2022) to study, at high temporal resolution, early colonization and succession on whale-bone and wood-fall habitat islands at 890-m depth in Barkley Canyon in the northeast Pacific Ocean. Our study site in Barkley Canyon falls within the Oxygen Minimum Zone (OMZ) of the NE Pacific, with bottom-water oxygen concentrations averaging less than 0.3 ml l-1 (De Leo et al., 2017; Chauvet et al., 2018), i.e., below the severe hypoxia threshold (0.3 – 0.5 ml l-1) associated with reductions in benthic macrofaunal and megafaunal diversity at many bathyal sites (Levin, 2003; Domke et al., 2017). Previous studies of whale bones and wood-falls at oxygen levels of 0.5 - 0.7 ml l/1 document rapid colonization of bones/wood by bone/wood borers and diverse faunal communities (e.g., Voight, 2007; Lundsten et al., 2010a; Glover et al., 2013; Young et al., 2022; Pereira et al., 2022). In addition, these bone/wood falls pass through the successional stages described above. Thus, our studies in Barkley Canyon allow us to explore whether community structure and succession on whale bones and wood may exhibit oxygen-sensitivity thresholds similar to those of other deep-sea benthic macrofaunal and megafaunal communities.

Our study design compares colonization patterns on three similarly sized substrates: organic-rich humpback whale bone, Douglas fir, and an inorganic control substrate, a carbonate rock. With seafloor cameras and ancillary oceanographic sensors connected in real time through Ocean Networks Canada's NEPTUNE Cabled Observatory, we conducted a standard, high-frequency routine of video observations on the implanted experimental substrates inside Barkley Canyon over an 8.3-month period. Following the 8.3-month period (after our video system was damaged by a bottom trawler), we conducted opportunistic observations of the colonization and degradation of our experimental substrates over the subsequent 8.5 yr using ROV imaging.

This experiment is part of a broader comparative experimental approach using whale-bone bone and wood substrates to evaluate bathymetric, regional and inter-ocean variations in biodiversity and connectivity, as well as interactions between biodiversity and ecosystem function, in whale-bone and wood-fall habitats at the deep-sea floor (Young et al., 2022). Our goal in this study is to elucidate, at high temporal resolution, the initial phases of colonization and succession of megafauna (animals > 1 cm, visible in imagery) on wood, whale-bone and carbonate substrates in a hypoxic bathyal habitat. During an 8.3-month period, we addressed the following specific questions:

1. How do megafaunal species abundances, total community abundance, species diversity and community structure vary over time on each substrate (whale bone, wood, and carbonate)?
2. Are megafaunal community temporal patterns (e.g., dominant species, and trends and frequencies of variation) similar across substrate types?
3. Are megafaunal community patterns correlated with key near-bottom and sea-surface environmental variables, in particular bottom-water oxygen concentration, temperature, current velocity, turbidity and chlorophyll-a concentrations, and near-surface ocean color (proxy of particulate organic matter/phytodetritus input)?

2 Materials and methods

2.1 Study area

Barkley Canyon is a shelf-incising submarine canyon located ~100 km west of Vancouver Island in the NE Pacific (Figure 1). It possesses multiple head branches intersecting the continental shelf, all discharging into the main canyon axis at mid-slope depths of 400–600 m (Figure 1). Barkley Canyon's seafloor between 350 to 2000 m provides a range of benthic habitats with distinct biological communities (Campanyà-Llovet et al., 2018; Domke et al., 2017). At mid-canyon depths near ~1000 m, hydrate outcrops with methane-seep communities (vesicomyid clam beds and bacterial mats) occur near a plateau on the canyon's northern flank (Thomsen et al., 2012; Riedel et al., 2022), with sparse cold-water coral communities occurring only a few hundred meters to the southeast (De Leo et al., 2024). The seeps are surrounded by bioturbated soft sediments, with megabenthic communities dominated by tanner crabs (*Chionoecetes tanneri*), buccinid gastropods (*Neptunea pacifica*), sablefish (*Anoplopoma fimbria*), and Pacific hagfish (*Heptatretus stoutii*) (Juniper et al., 2013; Seabrook et al., 2018, 2019).

Permanent hypoxic conditions, with dissolved oxygen concentrations below 0.5 $ml.l^{-1}$ (Diaz and Rosenberg, 2008; Vaquer-Sunyer and Duarte, 2008), occur between 870 and 970 m in Barkley Canyon (m=0.288; sd=0.017), with concentrations as low as 0.23 ml l^{-1} (Ocean Networks Canada's 12-yr time-series of observations). The low oxygen values coincide with the core of the oxygen minimum zone (OMZ) along this portion of the Cascadia Margin (De Leo et al., 2017), and appear to be an important driver of reduced megabenthic abundance and diversity in the canyon (Chauvet et al., 2018; Domke et al., 2017) and on the adjacent slope (De Leo et al., 2017).

Our study utilized Ocean Networks Canada's seafloor cabled observatory infrastructure installed in the Barkley Canyon Wall

(BCW) location at 870 m depth on soft sediments (De Leo et al., 2018), about 500 m from the nearest methane seep (Figure 1). The observatory installations allowed real-time monitoring with a high-definition video camera system in combination with standard oceanographic sensors, which have been measuring core essential ocean variables (e.g., temperature, salinity, pressure, dissolved oxygen, turbidity, current speed and direction) at 1-Hz frequency since May 2009 (Barnes et al., 2010; De Leo et al., 2018).

2.2 Experimental design, deployment and automated observation routine

On May 13 2014, three fresh-frozen and thawed adult humpback whale (*Megaptera novaeangliae*) cylindrical rib sections which had the bulk of flesh removed (each ~10-cm diameter and 30-cm long), one 20 x 20 x 10 cm block of untreated Douglas Fir wood (*Pseudotsuga menziesii*), and a ~30 x 30 x 30 cm block of authigenic carbonate (retrieved from a methane seep ~1000 m deep on the Costa Rica margin in 2009) were placed by a remotely operated vehicle (ROV) at 890 m depth near the northern wall of Barkley Canyon (Figure 1). All substrate packages were mounted on 35.5 x 35.5 cm, high-density PVC plates 20 cm above the seafloor on fiberglass grating, and positioned ~1 m from each other and about 50 cm concentrically from a high-definition video camera connected to ONC's cabled observatory (Figure 1C). Over a period of 8.3 months, 5-minute videos were recorded at 2-hr intervals. The camera system was mounted at a height of 65 cm above the seabed on a stainless-steel tripod frame with a ROS-485 Pan and Tilt (PT) unit. This allowed panning of the camera to each of the three substrates, and then holding position for at least 1 min during video recording. Two dimmable ROS LED lights

FIGURE 1
Benthic colonization and succession experiment study area in Barkley Canyon. **(A)**, deployment location in the NEPTUNE cabled observatory. **(B)**, Seafloor observatory infrastructure. **(C)**, photograph taken by the ROV Ocean Explorer during deployment showing experiment configuration. **(D-F)**, whalebones, wood and carbonate substrates images from the observatory seafloor video camera. Experiment plates are 30 x 30 cm in size.

(100 W, > 406 lm) provided illumination during video recording, and parallel laser beams 10-cm apart provided scaling. The 5-min recording/lights-on,1:55-h off schedule used is the standard for all video cameras installed on NEPTUNE's Barkley Canyon observatory node, and is intended to limit behavioral artifacts in deep-sea organisms exposed to artificial lighting (Robert and Juniper, 2012). The standardized and automated routine of video recordings was started on May 16 at 00:00:00 hrs (UTC), 3 days after the experiment was deployed by the ROV. ONC's online SeaTube Pro video player web interface (https://data.oceannetworks.ca/SeaTube) was used for performing video annotations. Animals were identified to the lowest possible taxonomic level and counts were performed from 30 s video segments from the 5-min videos at 2 different frequency intervals: 1) every 6 hours for the first 30 days, and 2) every 12 hours for the next 7.3 months. Only animals above the experiment plates were counted. Animals down to a length of ~1 cm (i.e., megafauna) could be identified. The video time-series was abruptly interrupted on January 12, 2015, ~8.3 months after the initial experiment deployment, when the Barkley Node subsea infrastructure was damaged by a bottom-trawling vessel. After this interruption, we used ROV video surveys to qualitatively assess multi-year trends in colonization by ecosystem engineers (i.e., *Osedax* sp., and *Xylophaga* sp.), bone/wood substrate degradation, and occurrence of bacterial mats. One of the three whale-bone rib sections was recovered on May 15 2016 (2 yr), a second one on August 1, 2018 (4 yr 3 mo), and the third and final along with the wood block were recovered on July 16 2023, after 9.2 years on the seafloor. Recovered bones and wood were frozen and examined under a compound microscope to assess the presence of *Osedax*/*Xylophaga*.

2.3 Quantifying bacterial-mat growth on whalebones

Bacterial-mat development on the whalebones was quantified from video frame grabs extracted at 72 h intervals for the entire 8.3 mo high-resolution observation period. The coverage of bacterial mats, identified as bone area covered by white filaments, was measured in square pixels using the masking tool in the post-processing image analysis software Image J (Schneider et al., 2012). No Bacterial mats were evident on the wood and carbonate substrates.

2.4 Monitoring of sea-surface and near-seabed environmental conditions

Co-located oceanographic instruments with sensors ~1.5 m above the seafloor, including a Sea-Bird Conductivity-Temperature-Depth-Dissolved Oxygen (CTD-O) sensor, a 2 MHz Nortek Aquadop Acoustic Doppler Profiler (ADCP), and a Wet Labs Eco FLNTU fluorometer/turbidity optical sensor, allowed the measurement at 1-Hz of the following environmental variables: bottom-water temperature (°C), salinity (PSU), dissolved oxygen concentration ($ml.l^{-1}$), horizontal current velocity (u, v, $m.s^{-1}$), acoustic backscatter (db), chl-a fluorescence ($mg.l^{-1}$) and turbidity (nephelometric turbidity units, NTU). All oceanographic data streams used in this paper are freely available for download at: https://data.oceannetworks.ca/DataSearch (search tree path: Pacific>Northeast Pacific>Barkley Canyon>MidWest and > MidEast).

Sea-surface environmental variability during the study period was assessed from long-term data available from the La Perouse Bank meteorological buoy station (C46206, latitude 48°50'24"N, longitude 126°00'00"), 60 km to the NE of the study site. The buoy is maintained by Environment and Climate Change Canada (ECCC), and data are accessible through the US National Oceanographic and Atmospheric Administration (NOAA) National Data Buoy Center (NDBC) (https://www.ndbc.noaa.gov/station_page.php?station=46206). Variables utilized were sea-surface temperature (°C), atmospheric pressure at sea level (dbar), significant wave height (m) and period (s), and wind speed (m/s) and direction. In addition, 8-day average ocean surface color data from the MODIS satellite, integrated over an area of 144 km^2 centered above our study site, were used as a proxy for surface primary productivity, following the same approach as Chauvet et al. (2018). Data were obtained from the NASA Earth Observations (NEO) Goddard Ocean Colour Group (https://modis.gsfc.nasa.gov/) and processed using SeaDAS data analysis software (Stramska, 2014).

2.5 Statistical analysis

2.5.1 Community succession and long-term trends in species diversity

Individual taxa were counted from videos on each experimental substrate, and 48-h running means of species abundance, total community abundance, species number, and the alpha-diversity indices Shannon's diversity (H') and Pielou's evenness (J) were calculated. Over the entire 8.3 mo experimental period, beta diversity, which is a good indicator of species turnover and community succession on time-series studies (Chu et al., 2018), was estimated for each substrate, as the total community composition variance (BD_{TOT}) using the respective abundance data matrices after Hellinger transformation (Legendre and De Cáceres, 2013). BD_{TOT} is then partitioned into the local (i.e. temporal sampling unit) contribution to beta diversity (LCBD) from each time point, representing the degree of uniqueness in terms of species composition, and also into the individual species' contributions to beta diversity (SCBD) over the entire 8.3 mo observation period (Legendre and De Cáceres, 2013). The value of the local contribution to beta diversity (LCBD) indicates the relative contribution of each observation to beta diversity, with high LCBD values identifying periods when the community composition changed. Alpha and beta diversity indices were calculated using the R packages "vegan" and "adespatial" (Oksanen et al., 2019; Dray et al., 2020). Correlations between the abundances of *Orchomenella obtusa* in different substrates were calculated with the nonparametric Kendall rank correlation test.

Whittaker-Robinson (WR) periodograms were used with 24-hr means to identify significant periodicities in changes of faunal

abundances over time for each of the experimental substrates (Whittaker and Robinson, 1923). Gaps in the abundance data (e.g., missing video recordings or poor imagery quality) were filled using K-nearest neighbor modeling using the function kNN of package VIM (Kowarik and Templ, 2016). All species abundance time series were tested for stationarity and, if found non-stationary, were detrended by computation and retention of regression residuals. The periodogram computation was completed using the function '*WRperiodogram*' from the R package "adespatial" (Dray et al., 2020), with significant periods identified at a confidence level of 5%. Since this analysis can lead to harmonics of periods also being highlighted, the periodogram calculates a maximum period of n/2; in this study, ~ 244 days.

Community trajectory analysis (CTA) (De Cáceres et al., 2019; Sturbois et al., 2021) was conducted to quantify temporal community variation within the three substrates. CTA was performed on the 48-h running means of species abundance using Nonmetric Multidimensional Scaling (nMDS) to compute the trajectories. Data was log(p+1) transformed and nMDS was performed using percentage difference (Bray-Curtis) dissimilarities and the R package "vegan" (Oksanen et al., 2019). Analysis of trajectories convergence and directionality were carried out using the package "ecotraj" (De Cáceres et al., 2019). Correlation between bacterial-mat coverage and trajectory segment lengths was tested for the whale bones using the Kendall rank correlation.

A Principal Response Curves (PRC) analysis was then applied to the community data to explore responses across treatments (in our case, substrate type) and time (van den Brink and ter Braak, 1999). PRC is a modified version of redundancy analysis (RDA) that plots the first principal component of the treatment effects by time, and compares the treatment effects against a "control" treatment. Carbonate, which lacked substantial organic enrichment, was used as the control treatment for the analysis, and data were log transformed prior to the analysis.

2.5.2 Environmental correlates of community succession at multiple time scales

In order to assess temporal structure in benthic communities on each experimental substrate and the potential role of environmental variables as drivers, a distance-based Moran's eigenvector maps (dbMEM) analysis was performed (Borcard et al., 2004; Legendre and Legendre, 2012). A dbMEM is a type of spatial eigenfunction analysis, adapted from spatial ecology to temporal analysis (Legendre and Gauthier, 2014), that computes eigenvectors of spatial configuration matrices and uses them as predictors in linear models. Because the fauna was sampled at different frequencies throughout the study period, abundance data and environmental variables were averaged for each day to create equal-sized sampling units throughout the experiment. The species-response data were Hellinger transformed and used to calculate the Euclidean distance. Then, response data were analyzed for linear trends using redundancy analysis (RDA) for each substrate separately, with only the detrended data kept for further analysis.

The matrix of Euclidean distance was constructed using a vector of dates to calculate eigenvectors (dbMEMs) using the function dbMEM of R package "adespatial". Only dbMEMs with positive Moran's I values were retained for further analysis. RDA (redundancy analysis) was conducted on the +dbMEM eigenvectors and the Hellinger-detrended abundance data for each substrate to measure variations in community structure that are explained as temporal structure. Significant +dbMEMs were selected via forward selection with a double stopping criterion (Blanchet et al., 2008), which allows the isolation of the dbMEMs that provide the most explanatory power. The significant dbMEMs were grouped visually in sub-models at distinct spatial scales (broad, medium, fine) by visually inspecting their sinusoidal periods and by using a scalogram to identify groupings of significant dbMEMs. RDAs were used to test the significance of each sub-model and a Whittaker–Robinson periodogram was used to determine their significant periods (Matabos et al., 2014). The environmental variables that contributed most to explaining the species abundance patterns (per substrate, separately) were also obtained via forward selection. The significant axes of the dbMEM model were then fitted using a linear regression or RDA to identify the significant contribution of the selected environmental variables in each sub-model. Variation partitioning was conducted using the response data, and the four explanatory datasets: (1) the forward selected environmental variables, (2) the linear trend, representing simpler temporal trends in the data, and (3) broad and (4) medium dbMEM temporal components, representing more complex temporal trends. A Venn diagram was created to display the results of the variation partitioning.

3 Results

3.1 Patterns of faunal abundance and diversity on individual substrates

A total of 10 faunal taxa were observed across all substrates (Table 1), with a total of 4650, 5576 and 4877 observations of faunal

TABLE 1 List of species observed and their relative contributions to temporal beta diversity (SCBD) on each experimental substrate in terms of the total beta diversity (BDTOT).

	Whale bone	Wood	Carbonate
Buccinum virridum	0.00	0.00	0.048
Orchomenella obtusa	0.514	0.720	0.804
Munidopsis quadrata	0.0069	0.024	0.0433
Chionoecetes tanneri	0.028	0.025	0.0282
Paralomis verrilli	0.00	0.00	0.049
Heptacarpus sp.	0.4384	0.2497	0.0520
Pandalopsis sp.	0.003147	0.0039	0.00
Anoplopoma fimbria	0.00	0.00	0.0077
Licenchelys sp.	0.00	0.00	0.0034
Eptatretus sp.	0.00923	0.00	0.007
BDTOT	0.137	0.160	0.038

individuals on whale bones, wood and carbonate, respectively, during the 8.3 mo (250 d) of high-frequency observations (see Supplementary Videos 1-3 for a quick overview of community succession over the 8.3 mo). Faunal colonists on all substrates over the 8.3 mo consisted of mobile species previously observed or collected (including by baited traps) in the surrounding community, with no evidence of bone/wood borers (i.e., decomposers) on bone/wood substrates.

Whale bones: Early colonization of whale bones was dominated by scavengers/omnivores. Multiple hagfish (*Eptatretus deani*), the low-oxygen-tolerant lysianassid amphipod *Orchomenella obtusa*, and shrimp (*Heptacarpus* sp.) were observed presumably feeding on the whale bones within the first five days (Figure 2A). Over the next 25-30 d, *Orchomenella obtusa* and *Heptacarpus* increased substantially in abundance, attaining peak levels of 16 and 93 individuals, respectively. Lysianassid amphipods remained the most abundant taxon on whale bones until ~45 d, and then declined rapidly as coverage by bacterial mats increased (Figure 2A). The abundance of *Heptacarpus* remained relatively stable from 30 d to 250 d, ranging up to 26 individuals. Colonization of whale bones by bacterial mats (dense white filaments) was first observed after three days, generally increased to a peak area near 140 days, and then declined to relatively stable lower levels from 170-250 d (Figure 2A; Supplementary Video 1). No evidence of bone-boring siboglinid worms in the genus *Osedax* (e.g., mucus sheaths, plumes, or bone borings) was observed on the whale bones over the entire 250-d period. Periodograms calculated from the 48-hr running averages of the two most abundant faunal species showed significant periods of 79 and 80 days only for *Orchomenella obtusa* (Supplementary Figure 1A; Table 2). Total faunal community abundance, also based on 48-h moving averages, peaked at ~80 individuals at ~35 days, while species richness peaked at 3 species after about ~12 d (Figures 3A, B). Alpha diversity on whalebones, as measured by Shannon H' and Pielou's J, showed initial peaks during the first~10 days, then decreased to about 40 d, and then increased to relatively constant values for the rest of the observation period (Figures 3C, D).

Approximately yearly ROV video monitoring of the whale bones following the 8.3 mo of high-frequency observations, as well as microscopic examination of recovered bones, indicated no colonization by *Osedax* of whale bones over a total period of 9.2 y (Supplementary Figure 3). Bacterial mats persisted on the bones from 8.3 mo to 9.2 y, but areal coverage of mats on bone surfaces declined as sediment and brown hydrozoans accumulated to cover some areas of the bones (Supplementary Figure 3). *Heptacarpus* sp. continued to be present at low abundances on the bones throughout the 9.2 y of the study.

Wood Substrate: Orchomenella obtusa and *Heptacarpus* sp. occurred in the first observation at 3 d. *Orchomenella* then increased rapidly to a secondary peak of ~50 individuals at 30 d, declined to zero

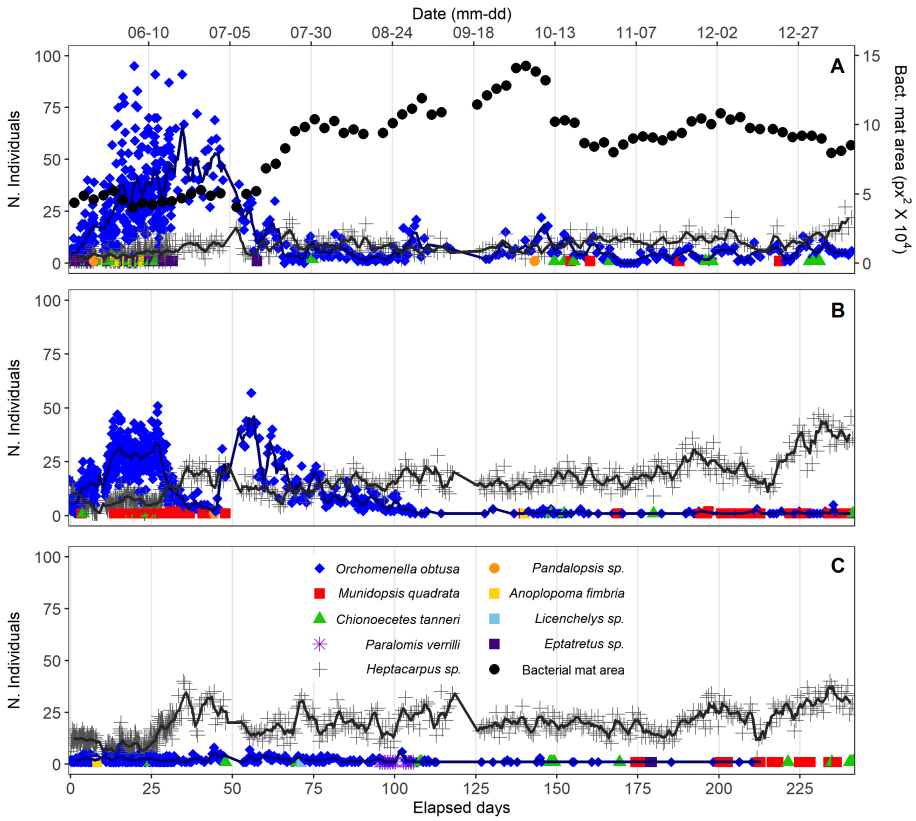

FIGURE 2
Individual counts of animal species >1 cm in length observed from 30-s video clips (**A**, whale-bones; **B**, wood, **C**, carbonate). Solid lines represent 48-h running means of the two most abundant species, *Orchomenella obtusa* and *Heptacarpus* sp.

10.3389/fmars.2024.1464095

TABLE 2 Results of Whittaker-Robinson periodogram analysis, identifying dominant periods for major species on whale-bone, wood and carbonate substrates.

Major species	Linear trend	Detrend	# Sig. periods	Sig. period (days)
Orchomenella obtusa				
Whalebones	$p < 0.001$	yes	2	79, 80
Wood	$p < 0.001$	no	15	62-68, 71-72, 111, 113-114, 116-118
Carbonate	$p < 0.001$	yes	4	61, 70, 102, 106
Heptacarpus sp.				
Whale bones	$p < 0.001$	yes	0	–
Wood	$p < 0.001$	yes	5	35-37, 44-45
Carbonate	$p < 0.001$	no	9	35-38, 72-76

abundance at ~48 d, then built up rapidly to a maximum of 57 at 59 d, and then gradually declined to essentially zero levels by 118 d (Figure 2B). *Heptacarpus* sp. very gradually increased from low abundance at ~30 d to a peak of 38 individuals at 243 d. Other species (*Munidopsis quadrata*, *Chionoecetes tanneri*) occurred as singletons or doubletons early (<51 d) and late (>150 d) in the 8.3 mo high-frequency observation period. No evidence of the wood-boring bivalve *Xylophaga*, such as siphons, borings,or feces, was observed at any time over the initial 8.3 mo. Periodograms showed significant periods for both *O. obtusa* between 60-75 and 110-120 days, and for *Heptacarpus* sp. between 34-36 and 45-46 days (Supplementary Figure 1B; Table 2). Community abundance based on 48-h moving averages showed secondary peaks of ~45 individuals at ~12 d and 215 d, with a primary maximum of ~60 inds. at ~60 d (Figure 3A). Species richness, also based on 48 h moving averages, peaked at 3 species around 25 d (Figure 3B). Shannon H' and Pielous's J were relatively high and constant during the first ~100 days, and then decreased to relatively low levels for the rest of the 8.3 mo observation period (Figures 3C, D).

Approximately yearly ROV video monitoring of the wood substrate following the 8.3-mo high-frequency observation period first revealed *Xylophaga* protruding from the wood block after 2 y (Supplementary Figure 4). Nonetheless, the wood remained largely intact, with sharp corners and only small boreholes visible, at least until 4.3 y. By 7.3 y, the wood block appeared to be losing its sharp corners apparently from *Xylophaga* boring (Supplementary Figure 4). Recovery of the wood substrate after 9.2 y revealed heavy riddling by *Xylophaga* borings, with very few live *Xylophaga* individuals remaining. From 4.3 y onward, the wood substrate became increasingly covered with brown hydrozoan colonies, achieving very heavy coverage with no visible gaps by 7.3 y (Supplementary Figure 4). *Heptacarpus* persisted at low abundance on the wood substrate throughout the 9.2 y of observations.

Carbonate Substrate: The shrimp *Heptacarpus* sp. was present on the carbonate on day three with three individuals, and increased in abundance to 40 inds. at ~38 d (Figure 2C). Abundances remained relatively high throughout the 250 d of high-frequency observations. The amphipod *O. obtusa* reached abundances of 7- 9 individuals at 18 - ~58 d, then generally occurred at lower abundances (2-4 individuals) to ~120 d, and then intermittently as singletons (Figure 2C). Several other species, including the lithodid *Paralomis verrilli*, the squat lobster *Munidopsis quadrata*, the crab *Chionoecetes tanneri*, and the zoarcid fish *Licenchelys* sp., occurred sporadically as singletons or doubletons on the carbonate block. Periodogram analysis showed significant periods for *Heptacarpus* sp. between 35-40 and 70-76 days and for *O. obtusa* for 60, 70, 100,105,110 days (Supplementary Figure 1C; Table 2). Total community abundance (48 h moving average) exhibited multiple peaks of 38-40 individuals throughout the 250 d (Figure 3A). Species richness (48 h moving ave.) peaked at 3 at ~100 days (Figure 3B). Shannon H' and Pielous's J on the carbonate substrate increased over the first 12 days, declined until ~25 days, and then remained relatively low compared to whale-bone and wood substrates (Figures 3C, D). During approximately annual ROV monitoring from 8.3 mo to 9.2 y, the carbonate substrate became increasingly colonized with brown hydrozoans, with most surfaces covered by 7.3 y. *Heptacarpus* sp. persisted at low to moderate abundance on the carbonate out to 9.2 y (Supplementary Figure 5).

3.2 Differences in faunal abundance and diversity between substrates

Early patterns of faunal diversity and abundance differed between the bone/wood substrates and the carbonate block. Colonization of bone and wood substrates within the first 50-60 days was dominated by the scavenger *O. obtusa*, but bone substrates supported higher amphipod abundance. Amphipod abundance on bone substrates declined rapidly after ~45 days coincident with rapid growth of bacterial mats on whale-bone surfaces (Figure 2A; Supplementary Video 1); this rapid decline on the bones coincided with an abrupt increase in *O. obtusa* on the wood. However, overall amphipod abundance was significantly correlated across bone and wood substrates ($\tau = 0.528$, $p < 0.001$). In contrast, *O. obtusa* abundance on the authigenic carbonate never attained high levels (Figure 2C), but was also significantly correlated with amphipod abundances on whale-bone ($\tau = 0.490$, $p < 0.001$) and wood ($\tau = 0.607$, $p < 0.001$) substrates. Furthermore, on the whale bones, community composition changed dramatically as bacterial mats became abundant at ~50 d (Figure 4). *Heterocarpus* remained more abundant on the wood and carbonate substrates from ~100 d to 250 d than on the whale bones (Figure 2).

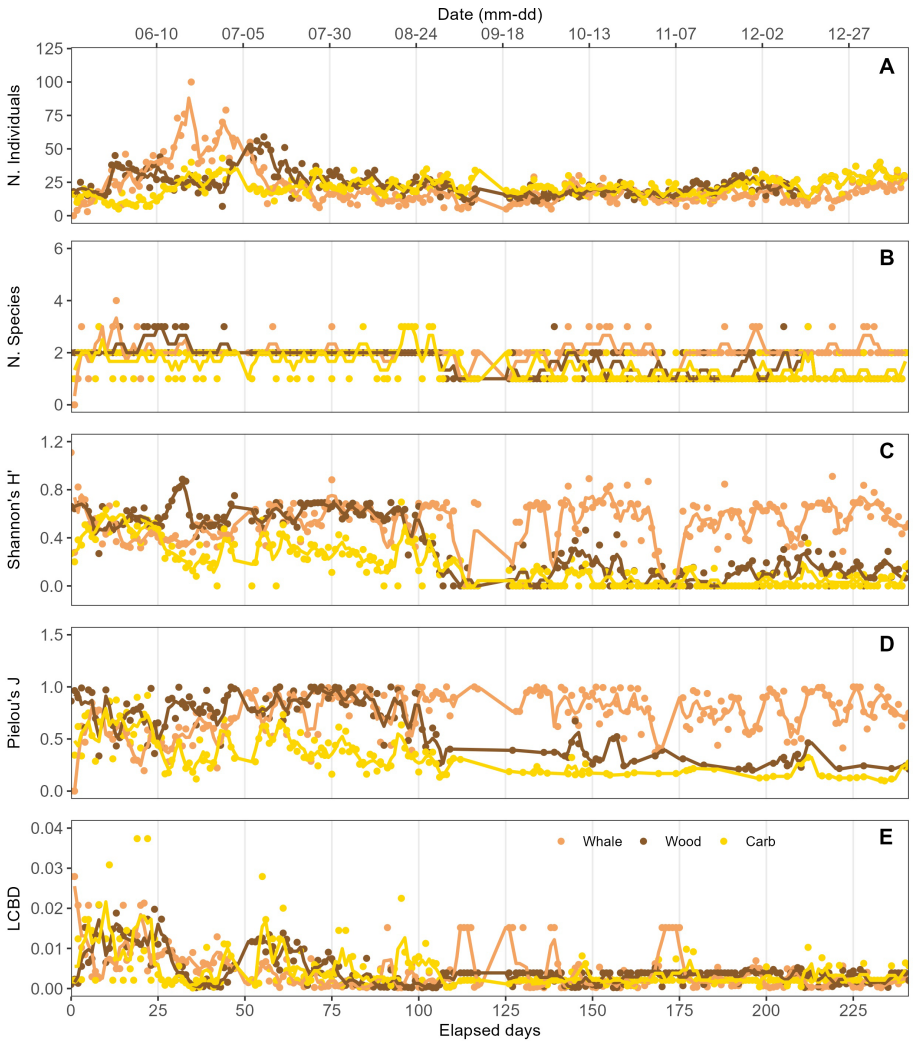

FIGURE 3
Total faunal abundance **(A)**, species richness **(B)**, Shannon Diversity **(C)**, Pielou's Evenness **(D)**, and beta-diversity (LCBD) **(E)**, based on individual counts on each substrate in each 30-sec video segment. Solid lines represent 48-h running means.

Remarkable changes in community composition, indicated by beta diversity analyses, occurred over the first months of the experiment on all three substrates, in particular in the first ~25 days. The LCBD time series identified a period (day 54-113) of gradual community changes toward stabilization on wood and carbonate substrates, while communities established on the whale bones experienced substantial variations until ~175 d (Figure 3E). The species contribution to the beta diversity index (SCBD) (Table 1) indicates the contribution of individual species to temporal variations in community composition. Among ten identified species, *O. obtusa* and *Heptacarpus* sp. made major contributions to temporal variations in community structure on whale-bone and wood substrates (Table 1). On the carbonate substrate, only *O. obtusa* made major contributions to beta diversity, with much higher SCBD value changes compared to other species, indicating its importance in driving community heterogeneity (Table 1). Total beta diversity (BD_{TOT}) values (Table 1), suggest that communities on bone and wood varied more over time than on the carbonate substrate.

Community Trajectory Analysis (CTA) indicate largely directional dissimilarity changes in wood and carbonate communities (Figure 4 - from left to right in the nMDS plots), with both communities converging at the end of the observation period (τ = -0.476, p = <0.001; Mann-Kendall test). Whale-bone communities exhibited directional change for the first ~120 days, but then lapsed into large, multidirectional changes, and diverged from wood (τ = 0.396, p = <0.001) and carbonate communities (τ = 0.140, p = <0.001). Trajectory lengths (L) were higher and directionality (DIR) was lower in the whale-bone substrate (L = 56.3, DIR = 0.393) compared to wood (L = 18.6, DIR = 0.533) and carbonate (L = 17.4, DIR = 0.501). Kendall rank correlation shows a positive trend (τ = 0.284, p = <0.001) between step lengths and bacterial-mat area on whale bones (i.e. when there was greater bacterial-mat coverage, the community was more dynamic).

Community responses clearly depended on the substrate ($_{adj}R^2$ = 0.597, p = 0.002) (Figure 5). During the first 110 days, the communities on the wood and whale-bone differed substantially from that on the carbonate. After 110 days, communities on wood and carbonate converged, while those on the whale-bone remained quite different. Early differences between bone/wood and carbonate appeared to be driven by the abundance of *O. obtusa*, while later

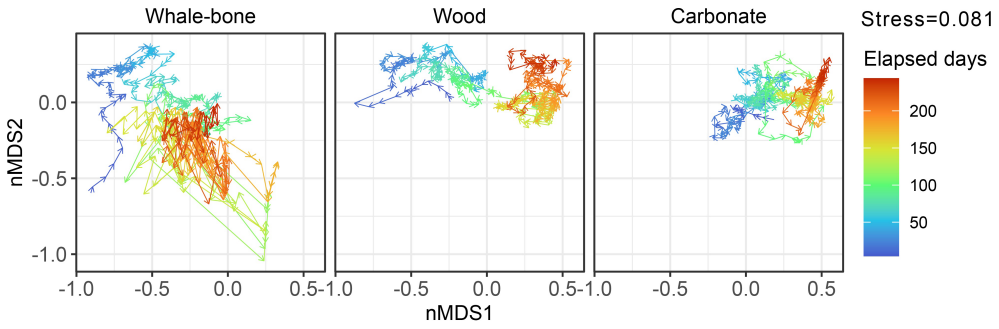

FIGURE 4
Trajectories of the faunal communities on whale-bone, wood, and carbonate substrates on the same nMDS space. Abundance data was log(p+1) transformed prior to non-Metric Multidimensional Scaling (nMDS) using percentage difference (Bray-Curtis) dissimilarities. Trajectories are colored by elapsed days, starting on May 16 2014 (dark blue) and ending on January 12 2015 (dark red).

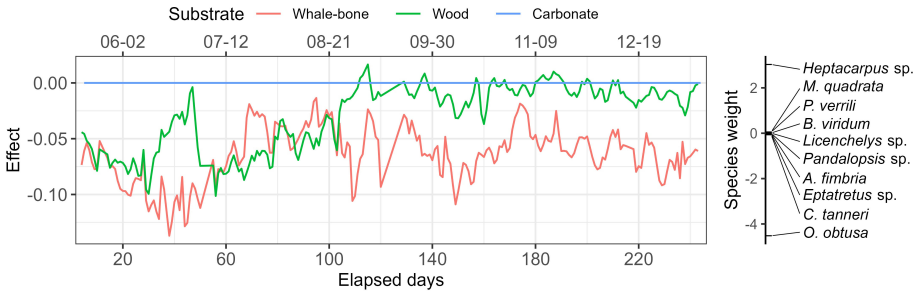

FIGURE 5
Principal Response Curves (PRC) of the colonization experiment study in Barkley Canyon Wall (BCW), showing the effect of each substrate in the community throughout the experiment and using Carbonate as a control treatment. Abundance data were aggregated using 48-hour running means obtained at 12-hour intervals and $\log_{p+1}$ transformed.

convergence between wood and carbonate appeared to be driven by relatively high abundances of *Heptacarpus* sp. (Figures 2, 5).

3.3 Environmental fluctuations at the seafloor and in surface waters

Environmental variables at ~1.5 m above the seafloor in Barkley Canyon are indicated at a 1-Hz frequency in Figure 6. Throughout the 250 d of observation, dissolved oxygen concentrations were severely hypoxic, ranging between 0.23 - 0.29 $ml.l^{-1}$, with a mean of 0.25 $ml.l^{-1}$ (sd = 0.01) (Figure 6A). Bottom-water temperatures had a mean of 3.82 °C (max=4.26, min=3.4, sd=0.12). Turbidity averaged 0.24 NTU (max=24.2, min=0.05, sd=1.2), and chlorophyll-a concentration averaged 0.08 $ug.l^{-1}$ (max=0.46, min=0.07, sd=0.01) for the entire period (Figure 6C) with each of these variables exhibiting a few, isolated high peaks. Current velocities averaged 7.5 $cm.s^{-1}$ (max=33.5, min=0.05, sd=1.2), in a predominantly southerly direction (Figure 6D). Acoustic backscatter at 1.2-2.0 m above the seabed, which tracked suspended particle load, averaged 30.5 dB (max=49, min=27.1, sd=2.16) (Figure 6E).

At the sea surface, winds, wave height, atmospheric pressure, and SST exhibited the expected strong seasonal changes characteristic of the NE Pacific (Figure 7). Wind speeds, which averaged 6 $m.s^{-1}$ (max=18.7, min=0, sd=3.5), significant wave height in meters (av=2.00, max=6.75, min=0.62, sd=1.10 m), and atmospheric pressure, in bars (av=1.01, max=1.04, min=0.98, sd=0.01), all exhibited enhanced variability during fall and winter months (Figures 7A–C). SST also followed a declining trend from summer to winter (av=13.3, max=17.7, min=9.5, sd=1.46). It is important to note that SST values were significantly higher, up to 3°C, than the 30-year average for the region, as our study period encompassed a severe and persistent marine heat wave, called 'The Blob' (Kintisch, 2015).

MODIS-Aqua chlorophyll, used as a proxy for sea-surface productivity, also showed strong temporal variability, ranging from 0.26 to 90 $mg.m^{-3}$, with highest values in spring and summer of 2013 (Figure 7D).

3.4 Environmental correlates of bone/wood/carbonate community succession

Communities established on all three substrates displayed significant linear trends. A total of 54 positive dbMEMs were calculated from the time distance matrix, which significantly explained the detrended community structure on all substrates (p = 0.001). Of those, between 14 and 18 dbMEMs per substrate were forward selected and used to model the faunal matrix

10.3389/fmars.2024.1464095

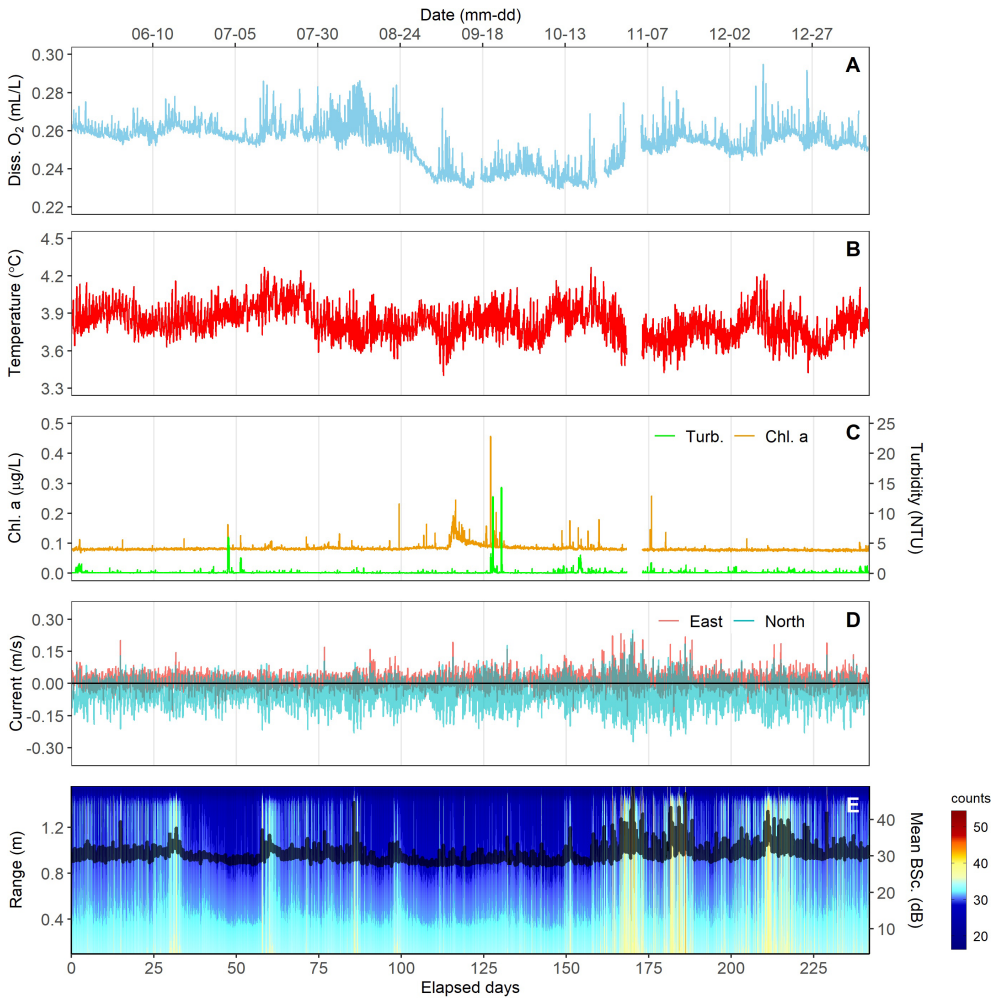

FIGURE 6
Oceanographic variables measured near the seafloor **(A)**, dissolved oxygen, **(B)**, temperature, **(C)**, Chl-a concentration and turbidity, **(D)**, current speed and direction (easterly and northerly directions are positive), and **(E)**, acoustic backscatter.

(Supplementary Figure 2). Most of the temporal structure in communities across all substrates was broad-scale (≥ 50 d periods), followed by medium scales (21-44 d) (Table 3; Supplementary Figure 2).

On whale bones, broad and medium variations in community structure were significant and explained 28.4% and 15.7% of the total variance, respectively (Table 3; Supplementary Figure 2). On the wood block, greater proportions of the variation in community structure were explained by broad and medium temporal scales: 46.2% and 21.5%, respectively. Broad scales also explained a high amount of variation in the community on the carbonate (21.3%), while medium (6.4%) and fine (2.2%) scales explained very small amounts.

Variations in community structure were also correlated with environmental variables at different time scales (Table 3, third line; Supplementary Figure 2). The variation explained by environmental variables never exceeded 0.35, indicating that biological processes (or unmeasured environmental variables), as opposed to the measured environmental variables, may play a bigger role in driving community patterns.

Significant explanatory variables show similarities and differences among the three substrate sub-models (Table 3 lines 5 - 15; Supplementary Figure 2). For all three substrates, temperature and chlorophyll explained significant variation in medium-scale temporal patterns, whereas salinity and SST were related to broad-scale patterns. Oxygen was only significantly related to broad-scale patterns for Wood and Carbonate. There is also evidence that sea-surface variables, especially SST and Along-slope wind, were related to variations in the community structure on bone and wood substrates. The environmental and temporal variables explained 66.6% of the variation in the community on the whale-bone substrate (Figure 8). The environmental variables explained 28.8% of the variation, and most is also explained by broad dbMEM and linear trend (20.3%). The variation explained by temporal variables independently of the environment is 40.0%, which may be associated with unmeasured environmental variables or biotic processes. Wood was the substrate with the most explained variance in the community (89.5%). More than half of the variance that is explained by the environmental variables is also explained by broad dbMEM and linear trend (56.1%), and 23.2%

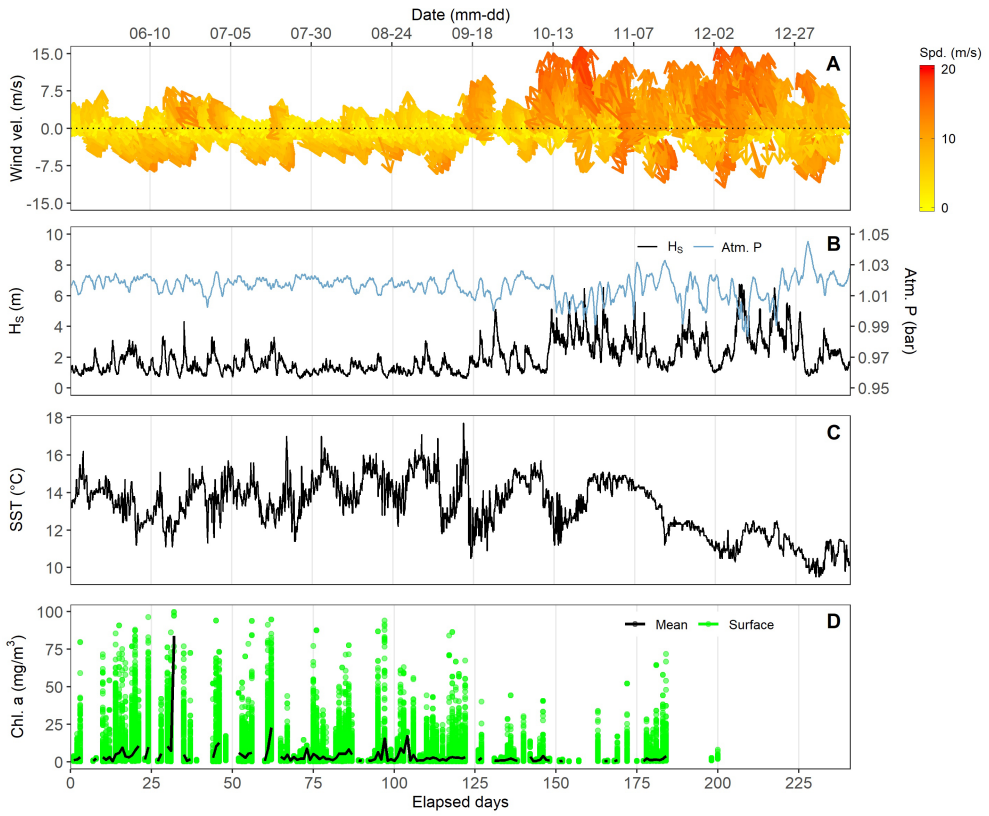

FIGURE 7
Climatological and oceanographic variables measured at the sea surface. **(A)**, wind velocity and direction; **(B)**, significant wave height (Hs), atmospheric pressure; **(C)**, sea surface temperature (SST); **(D)**, Surface chlorophyll derived from MODIS ocean color satellite data (mean and integrated over the entire study area, see Figure 1).

was explained by temporal variables independently of the environment. Similarly to the whale bones, the environmental and temporal variables explained 69.5% of the variation in the carbonate. However, the environmental variables explained most of the variation (52.3%) and 20.2% was explained by temporal variables independently of the environment, similar compared to the wood.

4 Discussion

4.1 Species and community patterns across substrates

Questions 1 and 2: Does community structure vary over time on whale-bone, wood, and carbonate, and, if so, are faunal-community temporal patterns similar across substrate types?

Faunal abundances, species diversity, and community structure varied substantially over the 250 d of high-frequency observations on each substrate, with markedly different patterns across substrates. Temporal changes on bones included (a) very high abundances of *O. obtusa* during the first ~50 d, and (b) abundant bacterial mats after this period. In contrast, wood sustained moderate abundances, and the carbonate low abundances, of these amphipods during the first 60 days, and both failed to develop visible bacterial mats (Figure 2). The abundance of *O. obtusa* on whale bones uniquely exhibited two significant periods of ~80 days; Early dominance by the mobile scavenging amphipod *O. obtusa* with a period of ~80 d likely reflects availability of soft tissue on the fresh whale bones. The later dominance by bacterial mats on the bones indicates the presence of sulfur-oxidizing bacteria utilizing sulfide produced by anaerobic bacterial decomposition of labile organic material on/in the whale bones (Smith and Baco, 2003; Smith et al., 2015). These changes suggest a rapid transition from a mobile scavenger stage to a sulfophilic stage of succession on the whale bones without an intervening enrichment opportunist stage characteristic of communities on intact whale carcasses (Smith and Baco, 2003; Smith et al., 2015). The absence of an enrichment opportunist stage likely results both from very limited availability of whale soft tissue on the whale bones at time of deployment and the absence of the bone-degrading worm *Osedax* over the 8.3 mo high-frequency observation period.

The wood community was also initially dominated by *O. obtusa*, but abundances were substantially lower than on the whale bones for the first ~60 days, yet still much higher than on carbonate (Figure 2). This pattern likely reflects intermediate levels of food availability for the scavenging amphipod on wood, i.e., much lower than on whale bones, but much higher than on the carbonate. Because the wood showed no evidence of wood-degrading *Xylophaga* bivalves or sulfur-oxidizing microbial mats

10.3389/fmars.2024.1464095

TABLE 3 Results from dbMEM analysis. R^2 and probabilities related to the temporal analysis of the colonization of whale-bone, wood and carbonate substrates.

	Whale-bone		Wood		Carbonate		
	Broad	Medium	Broad	Medium	Broad	Medium	Fine
Significant community periods	86-110	21-22	50-55	30-35, 42-44	54-60	21, 27-29	6-7
$_{adj}R^2$ dbMEM submodel on community	0.284	0.154	0.462	0.215	0.213	0.063	0.022
$_{adj}R^2$ environment on submodel	0.303	0.163	0.317	0.165	0.346	0.176	0.007
$_{adj}R^2$ environment on community	0.086	0.025	0.147	0.035	0.074	0.011	0.0001
Temperature		0.025*	0.028*	0.035*		0.068*	
Salinity	0.025*				0.131*		
Turbidity		0.020*		0.008			
Chlorophyll a		0.109*		0.080*		0.115*	0.011
Oxygen		0.009	0.152*		0.145*		
Along-slope current		0.012					
Cross-slope current					0.019*		
Upward current				0.011			
Acoustic backscatter			0.015*		0.040*		
Wave height							
Atmospheric pressure			0.016*				
SST	0.272*		0.107*	0.033*	0.015*		
Cross-slope wind	0.015*						
Along-slope wind		0.010*		0.020*	0.014*		

First line: Significant periods of each sub-model using a Whittaker–Robinson periodogram. Second line: Adjusted R^2 of each temporal sub-model. Third line: Adjusted R^2 of the regression of the sub-model (fitted values) on a subset of backward-selected environmental variables. Fourth line: product of the two previous lines, i.e., variation of the community data explained by the environmental variables. Other lines: R^2 values of the regression coefficients of the environmental variables on each submodel. *are coefficients with significant p-values.

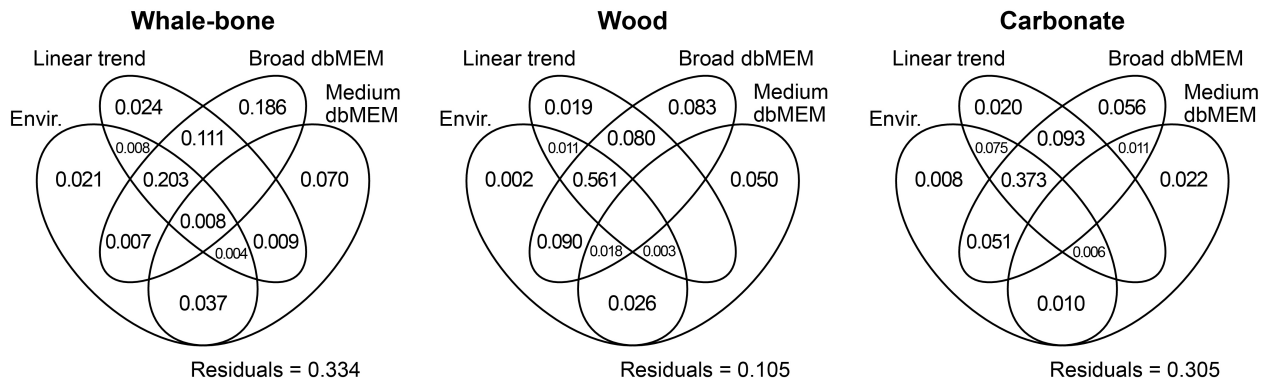

FIGURE 8
Venn diagram illustrating the result of variation partitioning of the colonization of whale-bone, wood, and carbonate with respect to environmental (Envir.) and temporal (linear trend, broad scale and medium scale positive dbMEMs) explanatory variables. The fractions of variation displayed in the diagram are computed from adjusted R^2. Circles are not drawn to scale.

during the 8.3 mo of high-frequency observations, an intermediate level of food availability on wood over this interval likely results from growth of cellulose-degrading microbes on the wood surfaces (Palacios et al., 2006, 2009; Fagervold et al., 2014; Hampel et al., 2022). Over the interval 50-75 days, as *O. obtusa* declined on whale bones, this amphipod abruptly increased in abundance on the wood to levels 2-3 fold higher than on the bones, and then gradually declined; we interpret this as a bone mass effect (sensu Leibold et al., 2004; Young et al., 2022) in which growing bacterial mats excluded large numbers of amphipods from the whale-bone surfaces, yielding

immigration to the wood block. Interestingly, the abundance of *O. obtusa* remained low on the carbonate throughout these 8.3 mo, exhibiting no substantial mass effect from the whale bones; we hypothesize that the carbonate provided little food for the scavenging amphipod and was much less desirable as a roosting location for amphipods feeding on the more organic-rich substrates of whale bones and wood (Smith, 1985).

Wood and carbonate communities also differed from those on whale bones by sustaining similar, higher abundances of *Heptacarpus* sp. for most of the 8.3 mo high-frequency observations (Figure 2). Species evenness declined and stabilized over time on wood and carbonate as these communities became increasingly dominated by *Heptacarpus* sp. (Figure 3). The shrimp appears to have been attracted to the physical structure of the wood and carbonate, and likely was excluded from bone surfaces by high concentrations of amphipods and microbial mats.

Communities on all three substrates showed directional changes in nMDS plots (Figure 4) over the first ~100 d, with wood and carbonate communities converging to a relatively stable, similar structure after 200 d, while the bone community exhibited substantial variations in community structure after 150 d as abundances of *O. obtusa, Heptacarpus* sp. and bacterial mats continued to vary. The greater trajectory length and lower directionality on bones compared to wood and carbonate likely reflects the initially higher food supply on bones (e.g, remnants of soft tissue), which attracted higher abundances of scavengers such as *O. obtusa* and *Eptatretus*. Bone-community divergence from wood and carbonate in latter stages likely is driven by the development of extensive microbial mats, and sulfide efflux, at bone surfaces.

Our qualitative ROV observations between 8.3 mo and 9.2 y (Supplementary Figures 3, 4) provide some insights into longer-term successional processes on our substrates. The persistence of microbial mats on our whale bones between 8.3 mo and 9.2 y indicates the presence of the sulphophilic stage on parts of the bones for 9.2 y, although colonization of hydroids in some areas suggest the bones are gradually transitioning to the final reef stage (Smith et al., 2015). The wood parcel appeared to be transitioning from the intermediate opportunist stage to the last senescence stage between 7.3 and 9.2 y (Pop Ristova et al., 2017).

There are few studies of co-located bone and wood at the deep-sea floor and these have focused on macrofauna. Young et al. (2022) also found that co-located whale-bone, wood, and rock substrates at the deep-sea floor at bathyal depths in the NE Pacific supported distinct macrofaunal communities. However, their study compared substrates after 15 mo at the seafloor and the bone/wood substrates were colonized by the ecosystem engineering taxa *Osedax*/*Xylophaga*. Similarly, Pereira et al. (2022) found different macrofaunal communities on *Xylophaga*-bored wood, cow bones (uncolonized by *Osedax)* and carbonate placed away from seepage for 7.4 y on the bathyal on the Costa Rica margin. Our results indicate that megafaunal community divergence can occur between bone and wood substrates even in the absence of *Osedax* and *Xylophaga*. Early divergence in our study was caused mainly by changes in species proportions and likely resulted from higher availability of labile organic matter on whale bones. Greater divergence between our bone and wood communities occurred with the development of microbial mats on the bones, indicative of the sulfophilic stage. We suggest that sulfate reducing bacteria within our whale bones, and within other whale falls (Smith et al., 2015; Alfaro-Lucas et al., 2017) also act as ecosystem engineers by anaerobically degrading bone lipids to provide a chemical energy source (sulfide) for mats of sulfur-oxidizing bacteria on the bones, producing a new reducing habit. This sulfide efflux may then exclude other biota such as scavenging amphipods and facilitate development of the sulfophilic stage of whale-fall community succession.

4.2 Environmental drivers of community structure

Question 3: Are faunal community patterns correlated with key near-bottom and/or sea-surface environmental variables?

Communities on all three substrates showed significant periods of temporal variability on broad (≥ 54 d) and medium (21- 29 d) time scales, and carbonate showed additional significant variability on fine (6-7 d) time scales, with ~ 30 - 35% of variability explained by measured environmental variables (Table 3). This suggests that biological processes, e.g., growth of microbial mats (or unmeasured environment variables), as opposed to the measured environmental variables, explain 65-70% of the observed community patterns in our study. The significant relationship between oxygen and broad-scale patterns in wood and carbonate communities, with ~15% of variability explained, and the lack of such a relationship for whale bones, indicates greater independence from oxygen variations in the whale-bone associated community. Lower sensitivity to reduced oxygen might be expected in whale-bone communities that persist in organic-rich whale-fall habitats (Smith et al., 2015). *Orchomenella obtusa*, in particular, has been shown to tolerate very low oxygen conditions to exploit food-rich habitats (De Robertis et al., 2001). In addition, chlorophyll-a, an index of phytodetritus availability (Thomsen et al., 2017), explained 8 to ~12% of medium-scale variability across all treatments. This suggests that phytodetritus may be a food source for many of the species observed in the study.

The amount of temporal variability explained in our study by environmental variables is comparable to levels of variability explained by environmental variables in similar time-series studies of benthic community dynamics on the bathyal NE Pacific margin (Matabos et al., 2014; Chauvet et al., 2018), but the partitioning of the variability was different. Only eight percent of the community variability at Barkley Canyon Axis (Chauvet et al., 2018) was explained by the combined effects of environmental parameters and temporal structure, and most of the variation was explained by the temporal model only (30%). For our wood and carbonate substrates, most of the variation was explained by the combined effects of environmental and temporal variables in the variation partitioning analysis, suggesting an important role of the environmental variables in these communities. In contrast, for the whale bones, much of the variation (40.3%) was explained by the temporal variables only, compared to 26.7% for environmental and temporal variables combined. This suggests that

biological processes (e.g., growth of microbial mats and/or interspecific relationships such as completion and predation) may be more important than physical drivers generally in controlling whale-bone megabenthic community structure over time scales of weeks to months.

It is noteworthy that we observed no colonization of the bone/wood substrates, or bone/wood degradation, by the ecosystem engineers *Osedax*/*Xylophaga* after 1.4 y, and no *Osedax* colonization or degradation of the bones even after 9.2 y. ROV images indicated some colonization of the wood by *Xylophaga* after 2 y, but any burrow-holes and siphons were very small and barely visible (Supplementary Figure 4). These rates of bone/wood colonization and degradation by *Osedax*/*Xylophaga* contrast sharply with rates in other bathyal settings with higher oxygen concentrations along the NE Pacific margin. For example, Lundsten et al. (2010a) found substantial *Osedax* colonization after six months on whale bones at 633 and 1018 m in Monterey Canyon (dissolved concentrations of 0.476 - 0.568 ml/l), and Smith et al. (2014) observed dense *Osedax* colonies on whale bones after 18 mo at oxygen levels of ~ 0.60 ml/l in Santa Cruz Basin (Juniper et al., 2021). Grupe (2014) observed 3 species of *Osedax* in whale bone after 1 year at Hydrate Ridge North off Oregon at ~600 m (0.34-0.52 ml/l O_2). *Osedax* was also reported on a whale skeleton at 1288 m on Clayoquot Slope (Lundsten et al., 2010b) where oxygen ranged annually from 0.33 - 0.57 ml/l over 10.8 years of observation from Sep 2013 to June 2024 (ONC Data Archive: https://data.oceannetworks.ca/PlottingUtility?refLink=Mjg0NjN8MTE4NDcHEQ).

For wood falls, Voight (2007) documented massive numbers of *Xylophaga* (including adults) and substantial decomposition in Douglas-fir blocks after 10 months on the Oregon margin at ~1500-2600 m depths with dissolved oxygen values of ~ 0.7 - 1.6 ml/l, and massive colonization was observed in Douglas-fir parcels after 6 mo in Santa Catalina Basin at 1240 m (shown in Glover et al., 2013) at 0.5 ml l^{-1}. of oxygen. The slow colonization of the wood by *Xylophaga* in our study apparently retarded community successional, since the development of the opportunistic stage depends on wood degradation by *Xylophaga* (Pop Ristova et al., 2017).

Slow to no colonization of *Osedax*/*Xylophaga* at our site could result from low-oxygen stress and/or from a lack of nearby larval sources. Reduced colonization rates seem unlikely to result from a lack of larval sources for *Xylophaga* since the west coast of Vancouver Island is heavily forested, yielding substantial wood inputs (Voight, 2007, 2009; Wohl and Iskin, 2021), and submarine canyons such as Barkley are known to accumulate wood debris and have been argued to be the preferred habitat for *Xylophaga* (Romano et al., 2013). For *Osedax*, a well developed whale-fall community with *Osedax* has been described ~90 km away on the Clayoquot Slope (Lundsten et al., 2010b). Furthermore, humpback and gray-whale migration routes and feeding grounds lie along the west coast of Vancouver Island (Calambokidis and Barlow, 2020; Carretta et al., 2020), yielding an abundant source of whales falls and potential larval sources for *Osedax* in the region. Given larval sources in the area, the along-axis currents in Barkley Canyon should facilitate larval transport across our experimental substrates (De Leo et al., 2018).

Thus, we hypothesize that no/slow colonization of *Osedax*/*Xylophaga* on our bone/wood substrates resulted from low-oxygen stress. Since oxygen levels fell to 0.22 ml/l during the 8.3 mo of our high-frequency observations, and *Osedax* has been observed at concentrations of 0.33 - 0.5 ml/l, this suggests an oxygen threshold for *Osedax* species in the region between 0.22 and 0.33 ml/l. Similarly, wood colonization and degradation by *Xylophaga* appears to be slowed by an oxygen threshold between 0.22 and 0.5 ml/l. These thresholds are similar to those of many macrofaunal and megafaunal taxa occurring near oxygen minimum zones (Levin, 2003; Chu and Tunnicliffe, 2015; Chu et al., 2018). Based on our results, we posit that OMZ expansion due to climate change, yielding increasing bathyal areas with oxygen concentrations between 0.22 and 0.33 ml/l (Levin, 2018; Breitburg et al., 2018; Sampaio et al., 2021) is likely to reduce habitat availability for bathyal *Osedax* and *Xylophaga*, and lower the decomposition rates of whale bones and wood on the NE Pacific margin. Other species that rely on these two engineering taxa to modify the substrate before they settle could also be affected.

Total megafaunal species richness on our whale bones (a maximum of four species at any time point) also is low compared to whale skeletons studied with similar video techniques in better oxygenated bathyal sites (9 - 45 taxa at any time point; Lundsten et al., 2010a, 2010b; Juniper et al., 2021). We think this also is partly related to oxygen stress; however, it may also be a function of the smaller size of the whale-bone habitat in our experiment compared to studies of entire whale skeletons (e.g., Lundsten et al., 2010b) because the areas of island habitats have been widely documented to be positively related to species richness (Ziegler et al., 2017).

Finally, it is also noteworthy that megafaunal community structure on our whale-bone, wood, and control treatments after 8.3 months was much more similar than observed for macrofauna on co-located whale-bone, wood and control substrates after 15 months in better oxygenated waters on the nearby Oregon-Washington margin (Young et al., 2022). Although there may be alternative explanations related to different faunal size classes and time intervals, we hypothesize that the lack of the ecosystem engineers *Osedax* and *Xylophaga*, in concert with oxygen stress, stymied the development of distinct whale-bone and wood-fall communities in Barkley Canyon compared to sites with higher oxygen availability (e.g., Bernardino et al., 2010; Lundsten et al., 2010a, 2010b; Young et al., 2022). Similarly, where active methane seepage apparently prevented colonization of *Osedax* and *Xylophaga*, the macrofaunal colonists of bone, wood and carbonate were very similar (Pereira et al., 2022). We thus posit that OMZ expansion will reduce the contribution of whale falls and wood falls to beta diversity on the NE Pacific margin.

Data availability statement

The datasets presented in this study can be found in online repositories. The names of the repository/repositories and accession number(s) can be found in the article/Supplementary Material.

Ethics statement

Ethical approval was not required for the study involving animals in accordance with the local legislation and institutional requirements because the whale bones were isolated as part of a previous study for which ethical approval for scientific research was obtained. Possession of the whale bones in the USA was authorized under NMML Permit No. 13583. Export of the whale bones to Canada was authorized under CITES Permit No. 14US30727B/9. The study was conducted in accordance with the local legislation and institutional requirements.

Author contributions

CS: Conceptualization, Formal analysis, Funding acquisition, Investigation, Methodology, Project administration, Resources, Supervision, Validation, Writing – original draft, Writing – review & editing. FDL: Conceptualization, Formal analysis, Funding acquisition, Investigation, Methodology, Project administration, Resources, Supervision, Validation, Writing – original draft, Writing – review & editing, Data curation. PC: Data curation, Formal analysis, Software, Validation, Visualization, Writing – review & editing. AG: Formal analysis, Visualization, Writing – review & editing. LL: Conceptualization, Resources, Writing – review & editing.

Funding

The author(s) declare financial support was received for the research, authorship, and/or publication of this article. Ocean Networks Canada is a non-profit initiative of University of Victoria, funded primarily by the Canada Foundation for Innovation, Major Science Initiative Fund 30199. This work was supported in part by US National Science Foundation grant # 1155703 to CS and received additional support from ONC's Enhanced Support Program 2018/2019.

Acknowledgments

We thank Ocean Networks Canada for shore and at-sea support devoted to the maintenance of the NEPTUNE cabled observatory. We thank the captain and crews of CCGS J.P Tully and EV Nautilus, and ROV pilots of Hercules and Ocean Explorer (Dave Tetarenko, *in memoriam*) for the precise deployment and handling of fragile colonization experiments. We also extend our gratitude to ONC's 'Data Analytics' and 'Data Stewardship' teams for ensuring data quality and curation of all observatory data streams utilized in this study. We especially thank M. Rankin, who helped in the preparation of maps for Figure 1, G. Garner for help with time-series plots, and L. Guan for faunal video annotations. We thank Dr. Pierre Legendre at University of Montreal for insights into the selection and interpretations of the Community Trajectory Analysis and Principal Response Curves. This is contribution 11849 from the School of Ocean and Earth Science and Technology, University of Hawaii at Manoa.

Conflict of interest

The authors declare that the research was conducted in the absence of any commercial or financial relationships that could be construed as a potential conflict of interest.

Publisher's note

Supplementary material

The Supplementary Material for this article can be found online at: https://www.frontiersin.org/articles/10.3389/fmars.2024.1464095/full#supplementary-material

SUPPLEMENTARY VIDEO 1
https://youtu.be/FsFE0gwwkQA.

SUPPLEMENTARY VIDEO 2
https://youtu.be/jJZ3xVAyK6g.

SUPPLEMENTARY VIDEO 3
https://youtu.be/rYQc8YSY7JY.

References

Aguzzi, J., Company, J. B., Costa, C., Matabos, M., Azzurro, E., Mànuel, A., et al. (2012). Challenges to assessment of benthic populations and biodiversity as a result of rhythmic behaviour: video solutions from cabled observatories. *Oceanography Mar. Biology: Annu. Rev.* 50, 235–286.

Aguzzi, J., Fanelli, E., Ciuffardi, T., Schirone, A., De Leo, F. C., Doya, C., et al. (2018). Faunal activity rhythms influencing early community succession of an implanted whale carcass offshore Sagami Bay, Japan. *Sci. Rep.* 8, 11163. doi: 10.1038/s41598-018-29431-5

Alfaro-Lucas, J. M., Shimabukuro, M., Ferreira, G. D., Kitazato, H., Fujiwara, Y., and Sumida, P. Y. G. (2017). Bone-eating *Osedax* worms (Annelida: Siboglinidae) regulate biodiversity of deep-sea whale-fall communities. *Deep-Sea Res. Part II* 146, 4–12. doi: 10.1016/j.dsr2.2017.04.011

Barnes, C. R., Best, M. M., Johnson, F. R., and Pirenne, B. (2010). Final installation and initial operation of the world's first regional cabled ocean observatory (NEPTUNE Canada). *Can. Met. Ocean. Soc.* 38, 89–96.

Bernardino, A. F., Smith, C. R., Baco, A., Altamira, I., and Sumida, P. Y. G. (2010). Macrofaunal succession in sediments around kelp and wood falls in the deep NE Pacific and community overlap with other reducing habitats. *Deep Sea Research Part I.* 57, 5, 708–723. doi: 10.1016/j.dsr.2010.03.004

Bienhold, C., Ristova, P. P., Wenzhöfer, F., Dittmar, T., and Boetius, A. (2013). How deep-sea wood falls sustain chemosynthetic life. *PloS One* 8, e53590. doi: 10.1371/journal.pone.0053590

Blanchet, F. G., Legendre, P., and Borcard, D. (2008). Forward selection of explanatory variables. *Ecology* 89, 2623–2632. doi: 10.1890/07-0986.1

Borcard, D., Legendre, P., Avois-Jacquet, C., and Tuomisto, H. (2004). Dissecting the spatial structure of ecological data at multiple scales. *Ecology* 85, 1826–1832. doi: 10.1890/03-3111

Breitburg, B., Levin, L. A., Oschlies, A., Grégoire, M., Chavez, F. P., Conley, D. J., et al. (2018). Declining oxygen in the global ocean and coastal waters. *Science* 359, (46) 1–(46)11. doi: 10.1126/science.aam7240

Calambokidis, J., and Barlow, J. (2020). *Update abundance estimates for blue and humpback whales along the U.S. west coast using data through 2018*, (San Diego, CA: NOAA technical memorandum NMFS-SWFSC-634, Olympia WA) Vol. 634. doi: 10.25923/zrth-8n96

Campanyà-Llovet, N., Snelgrove, P. V. R., and De Leo, F. C. (2018). Food quantity and quality in Barkley Canyon (NE Pacific) and its influence on macroinfaunal community structure. *Prog. Oceanography* 169, 106–119. doi: 10.1016/j.pocean.2018.04.003

Carretta, J. V., Forney, K. A., Oleson, E. M., Weller, D. W., Lang, A. R., Baker, J., et al. (2020). *U.S. Pacific Marine Mammal Stock Assessments: 2019* (U.S. Department of Commerce, National Oceanic and Atmospheric Administration National Marine Fisheries Service Southwest Fisheries Science Center - NOAA, Seattle, WA). https://repository.library.noaa.gov/view/noaa/29973.

Chauvet, P., Metaxas, A., Hay, A. E., and Matabos, M. (2018). Annual and seasonal dynamics of deep-sea megafaunal epibenthic communities in Barkley Canyon (British Columbia, Canada): A response to climatology, surface productivity and benthic boundary layer variation. *Prog. Oceanography* 169, 89–105. doi: 10.1016/j.pocean.2018.04.002

Chu, J. W. F., Curkan, C., and Tunnicliffe, V. (2018). Drivers of temporal beta diversity of a benthic community in a seasonally hypoxic fjord. *R. Soc. OpenScience* 5, 172284. doi: 10.1098/rsos.172284

Chu, J. W. F., and Tunnicliffe, V. (2015). Oxygen limitations on marine animal distributions and the collapse of epibenthic community structure during shoaling hypoxia. *Global Change Biol.* 21, 2989–3004. doi: 10.1111/gcb.12898

De Cáceres, M., Coll, L., Legendre, P., Allen, R. B., Wiser, S. K., Fortin, M. J., et al. (2019). Trajectory analysis in community ecology. *Ecol. Monogr.* 89, e01350. doi: 10.1002/ecm.1350

De Leo, F. C., Correa, P. V. F., Lo Iacono, C., and Corbera, G. (2024). "Black coral assemblages in Barkley Canyon, NE Pacific, in the vicinities of the NEPTUNE observatory: the role of internal waves, canyon topography and an oxygen minimum zone in shaping community structure," in *ASLO Ocean Sciences Meeting* (New Orleans). Available at: https://agu.confex.com/agu/OSM24/meetingapp.cgi/Paper/1491541.

De Leo, F. C., Gauthier, M., Nephin, J., Mihály, S., and Juniper, S. K. (2017). Bottom trawling and oxygen minimum zone influences on continental slope benthic community structure off Vancouver Island (NE Pacific). *Deep-Sea Res. II* 137, 404–419. doi: 10.1016/j.dsr2.2016.11.014

De Leo, F. C., Ogata, B., Sastri, A. R., Heesemann, M., Mihály, S., Galbraith, M., et al. (2018). High-frequency observations from a deep-sea cabled observatory reveal seasonal overwintering of Neocalanus spp. in Barkley Canyon, NE Pacific: Insights into particulate organic carbon flux. *Prog. Oceanography* 169, 120–137. doi: 10.1016/j.pocean.2018.06.001

De Robertis, A., Eiane, K., and Rau, G. H. (2001). Eat and Run: anoxic feeding and subsequent aerobic recovery by Orchomene obtusus in Sanich Inlet, British Columbia, Canada. *Mar. Ecol. Prog. Ser.* 219, 221–227. doi: 10.3354/meps219221

Diaz, R. J., and Rosenberg, R. (2008). Spreading dead zones and consequences for marine ecosystems. *Science* 321, 926–929. doi: 10.1126/science.1156401

Distel, D. L., Baco, A. R., Chuang, E., Morrill, W., Cavanaugh, C., and Smith, C. R. (2000). Marine ecology: Do mussels take wooden steps to deep-sea vents? *Nature* 403, 725–726. doi: 10.1038/35001667

Distel, D. L., and Roberts, S. J. (1997). Bacterial endosymbionts in the gills of the deep-sea wood-boring bivalves *Xylophaga atlantica* and *Xylophaga washingtona*. *Biol. Bull.* 192, 253–261. doi: 10.2307/1542719

Domke, L., Lacharité, M., Metaxas, A., and Matabos, M. (2017). Influence of an oxygen minimum zone and macroalgal enrichment on benthic megafaunal community composition in a NE Pacific submarine canyon. *Mar. Ecol.* 38, e12481. doi: 10.1111/maec.12481

Dray, S., Bauman, D., Blanchet, G., Borcard, D., Clappe, S., Guenard, G., et al. (2020). *adespatial: Multivariate Multiscale Spatial Analysis. R package version 0.3-8*. Available online at: https://CRAN.R-project.org/package=adespatial (Accessed December 03, 2023).

Fagervold, S. K., Romano, C., Kalenitchenko, D., Borowski, C., Nunes-Jorge, A., Martin, D., et al. (2014). Microbial communities in sunken wood are structured by wood-boring bivalves and location in a submarine canyon. *PloS One* 9, e96248. doi: 10.1371/journal.pone.0096248

Gessner, M. O., Swan, C. M., Dang, C. K., McKie, B. G., Bardgett, R. D., Wall, D. H., et al. (2010). Diversity meets decomposition. *Trends Ecol. Evol.* 25, 372–380. doi: 10.1016/j.tree.2010.01.010

Glover, A. G., Wiklund, H., Taboada, S., Avila, C., Cristobo, J., Smith, C. R., et al. (2013). Bone-eating worms from the Antarctic: the contrasting fate of whale and wood remains on the Southern Ocean seafloor. *Proc. R. Soc. B* 280, 20131390. doi: 10.1098/rspb.2013.1390

Gros, O., Guibert, J., and Gaill, F. (2007). Gill-symbiosis in mytilidae associated with wood fall environments. *Zoomorphology* 126, 163–172. doi: 10.1007/s00435-007-0035-3

Grupe, B. (2014). Implications of Environmental Heterogeneity for Community Structure, Colonization, and Trophic Dynamics at Eastern Pacific Methane Seeps. Scripps Institution of Oceanography, University of California, San Diego.

Hampel, J. J., Moseley, R. D., Mugge, R. L., Ray, A., Damour, M., Jones, D., et al. (2022). Deep-sea wooden shipwrecks influence sediment microbiome diversity. *Limnology Oceanography* 67 (2), 482–497. doi: 10.1002/lno.12008

I. Hanski and Y. Cambefort (Eds.) (1991). *Dung Beetle Ecology* (Princeton: Princeton University Press), 481.

I. A. G. Hanski and M. E. Gilpin (Eds.) (1997). *Metapopulation biology: Ecology, Genetics, and Evolution* (San Diego: Academic Press), 512.

Harbour, R. P., Smith, C. R., Fernandes, T. F., and Sweetman, A. K. (2021a). Trophic ecology surrounding kelp and wood falls in deep Norwegian fjords. *Deep Sea Res. Part I: Oceanographic Res. Papers* 173, 103553. doi: 10.1016/j.dsr.2021.103553

Harbour, R. P., Smith, C. R., Simon-Nutbrown, C., Cecchetto, M., Young, E., Coral, C., et al. (2021b). Biodiversity, community structure and ecosystem function on kelp and wood falls in the Norwegian deep sea. *Mar. Ecol. Prog. Ser.* 657, 73–91. doi: 10.3354/meps13541

Juniper, F., Jameson, B. D., Juniper, S. K., Smith, C. R., and Bell, L. S. (2021). Can whale-fall studies inform human forensics? *Sci. Justice* 61, 459–466. doi: 10.1016/j.scijus.2021.06.001

Juniper, S. K., Matabos, M., Mihály, S., Ajayamohan, R., Gervais, F., and Bui, A. (2013). A year in Barkley Canyon: a time-series observatory study of mid-slope benthos and habitat dynamics using the NEPTUNE Canada network. *Deep-Sea Res. II* 92, 114–123. doi: 10.1016/j.dsr2.2013.03.038

Kintisch, E. (2015). The 'Blob' invades Pacific, flummoxing climate experts. *Science* 348, 17–18. doi: 10.1126/science.348.6230.17

Kowarik, A., and Templ, M. (2016). Imputation with the R package VIM. *J. Stat. Software* 74, 1–16. doi: 10.18637/jss.v074.i07

Legendre, P., and De Cáceres, M. (2013). Beta diversity as the variance of community data: dissimilarity coefficients and partitioning. *Ecol. Lett.* 16, 951–963. doi: 10.1111/ele.12141

Legendre, P., and Gauthier, O. (2014). Statistical methods for temporal and space-time analysis of community composition data. *Proc. R. Soc B* 281, 20132728. doi: 10.1098/rspb.2013.2728

Legendre, P., and Legendre, L. (2012). *Numerical ecology. 3rd English Edition* (Elsevier).

Leibold, M. A., Holyoak, M., Mouquet, N., Amarasekare, P., Chase, J. M., and Hoopes, M. F. (2004). The metacommunity concept: a framework for multi-scale community ecology. *Ecol. Lett.* 7, 601–613. doi: 10.1111/j.1461-0248.2004.00608.x

Lelievre, Y., Legendre, P., Matabos, M., Mihály, S., Lee, R. W., Sarradin, P.-M., et al. (2017). Astronomical and atmospheric impacts on deep-sea hydrothermal vent invertebrates. *Proc. R. Soc. B* 284, 20162123. doi: 10.1098/rspb.2016.2123

Levin, L. A. (2003). Oxygen Minimum zone benthos: adaptation and community response to hypoxia. *Oceanography Mar. Biology: an Annu. Rev.* 41, 1–45.

Levin, L. A. (2018). Manifestation, drivers, and emergence of open ocean deoxygenation. *Annu. Rev. Mar. Sci.* 10, 229–260. doi: 10.1146/annurev-marine-121916-063359

Lundsten, L., Paul, C., Schlining, K. L., McGann, M., and Ussler III, W. (2010b). Biological characterization of a whale-fall near Vancouver Island, British Columbia, Canada. *Deep-Sea Res. I* 57, 918–922. doi: 10.1016/j.dsr.2010.04.006

Lundsten, L., Schlining, K. L., Frasier, K., Johnson, S. B., Kuhnz, L., Harvey, J., et al. (2010a). Time-series analysis of six whale-fall communities in Monterey Canyon, California, USA. *Deep-Sea Res. I* 57, 1573–1584. doi: 10.1016/j.dsr.2010.09.003

Matabos, M., Bui, A. O. V., Mihály, S., Aguzzi, J., Juniper, S. K., and Ajayamohan, R. S. (2014). High-frequency study of epibenthic megafaunal community dynamics in Barkley Canyon: A multi-disciplinary approach using the NEPTUNE Canada network. *J. Mar. Syst.* 130, 56–68. doi: 10.1016/j.jmarsys.2013.05.002

Menge, B. A., Sanford, E., Daley, B. A., Freidenburg, T. L., Hudson, G., and Lubchenco, J. (2002). Inter-hemispheric comparison of bottom-up effects on community structure: insights revealed using the comparative-experimental approach. *Ecol. Res.* 17, 1–16. doi: 10.1046/j.1440-1703.2002.00458.x

Oksanen, J., Blanchet, F. G., Friendly, M., Kindt, R., Legendre, P., McGlinn, D., et al. (2019). *vegan: Community Ecology Package. R package version 2.5-6*. Available online at: https://CRAN.R-project.org/package=vegan (Accessed November 08, 2023).

Pailleret, M., Haga, T., Petit, P., Privé-Gill, C., Saedlou, N., Gaill, F., et al. (2007). Sunken wood from the Vanuatu Islands: identification of wood substrates and preliminary description of associated fauna. *Mar. Ecol.* 28, 233–241. doi: 10.1111/j.1439-0485.2006.00149.x

Palacios, C., Zbinden, M., Baco, A. R., Treude, T., Smith, C. R., Gaill, F., et al. (2006). Microbial ecology of deep-sea sunken wood: quantitative measurements of bacterial biomass and cellulolytic activities. *Cahiers Biologie Mar.* 47, 415–420. doi: 10.21411/CBM.A.45C32F7B

Palacios, C., Zbinden, M., Pailleret, M., Gaill, F., and Lebaron, P. (2009). Highly similar prokaryotic communities of sunken wood at shallow and deep-sea sites across the oceans. *Microbial Ecol.* 58, 737–752. doi: 10.1007/s00248-009-9538-4

Pereira, O. S., Gonzalez, J., Mendoza, G. F., Le, J., Coscino, C. L., Lee, R. W., et al. (2021). The dynamic influence of methane seepage on macrofauna inhabiting authigenic carbonates. *Ecosphere* 12, e03744. doi: 10.1002/ecs2.3744

Pereira, O. S., Gonzalez, J., Mendoza, G. F., Le, J., McNeill, M., Ontiveros, J., et al. (2022). Does substrate matter in the deep sea? A comparison of bone, wood, and carbonate rock colonizers. *PloS One* 17, e0271635. doi: 10.1371/journal.pone.0271635

Pop Ristova, P., Bienhold, C., Wenzhöfer, F., Rossel, P. E., and Boetius, A. (2017). Temporal and spatial variations of bacterial and faunal communities associated with deep-sea wood falls. *PloS One* 12, e0169906. doi: 10.1371/journal.pone.0169906

Quaggiotto, M.-M., Sánchez-Zapata, J. A., Bailey, D. M., Payo-Payo, A., Navarro, J., Brownlow, A., et al. (2019). Past, present and future of the ecosystem services provided by cetacean carcasses. *Ecosystem Serv.* 54, 101406. doi: 10.1016/j.ecoser.2022.101406

Richer de Forges, B., Tan, S. H., Bouchet, P., Ng, P. K. L., Chan, T.-Y., and Saguil, N. (2009). PANGLAO 2005—survey of the deep-water benthic fauna of the Bohol Sea and adjacent waters. *Raffles Bull. Zool* 20, 21–38.

Riedel, M., Scherwath, M., Römer, M., Paull, C. K., Lundsten, E. M., Caress, D., et al. (2022). Barkley canyon gas hydrates: A synthesis based on two decades of seafloor observation and remote sensing. *Front. Earth Sci.* 10. doi: 10.3389/feart.2022.852853

Robert, K., and Juniper, S. K. (2012). Surface-sediment bioturbation quantified with cameras on the NEPTUNE Canada cabled observatory. *Mar. Ecol. Prog. Ser.* 453, 137–149. doi: 10.3354/meps09623

Rodriguez, E., and Daly, M. (2010). Phylogenetic relationships among deep-sea and chemosynthetic sea anemones: actinoscyphiidae and actinostolidae (Actiniaria: mesomyaria). *PloS One* 5, e10958. doi: 10.1371/journal.pone.0010958

Romano, C., Voight, J. R., Company, J. B., Plyuscheva, M., and Martin, D. (2013). Submarine canyons as the preferred habitat for wood-boring species of Xylophaga (Mollusca, Bivalvia). *Prog. Oceanography* 118, 175–187. doi: 10.1016/j.pocean.2013.07.028

Sampaio, E., Santos, C., Rosa, I. C., Ferreira, V., Pörtner, H. O., Duarte, C. M., et al. (2021). Impacts of hypoxic events surpass those of future ocean warming and acidification. *Nat. Ecol. Evol.* 5, 311–321. doi: 10.1038/s41559-020-01370-3

Schaetzl, R. J., Johnson, D. L., Burns, S. F., and Small, T. W. (1989). Tree uprooting: review of terminology, process, and environmental implications. *Can. J. For. Res.* 19, 1–11. doi: 10.1139/x89-001

Schneider, C. A., Rasband, W. S., and Eliceiri, K. W. (2012). NIH Image to ImageJ: 25 years of image analysis. *Nat. Methods* 9, 671–675. doi: 10.1038/nmeth.2089

Schoenly, K., and Reid, W. (1987). Dynamics of heterotrophic succession in carrion arthropod assemblages: discrete seres or a continuum of change? *Oecologia* 73, 192–202. doi: 10.1007/BF00377507

Seabrook, S., De Leo, F. C., Baumberger, T., Raineault, N., and Thurber, A. R. (2018). Heterogeneity of methane seep biomes in the Northeast Pacific. *Deep Sea Res. Part II: Topical Stud. Oceanography* 150, 195–209. doi: 10.1016/j.dsr2.2017.10.016

Seabrook, S., De Leo, F. C., and Thurber, A. R. (2019). Flipping for food: the use of a methane seep by tanner crabs (*Chionoecetes tanneri*). *Front. Mar. Sci.* 6. doi: 10.3389/fmars.2019.00043

Smith, C. R. (1985). Food for the deep sea: utilization, dispersal, and flux of nekton falls at the Santa catalina basin floor. *Deep-Sea Res. Part A* 32, 417–442. doi: 10.1016/0198-0149(85)90089-5

Smith, C. R., and Baco, A. R. (2003). Ecology of whale falls at the deep-sea floor. *Oceanography Mar. Biology: an Annu. Rev.* 41, 311–354.

Smith, C. R., Bernardino, A. F., Baco, A., Hannides, A. K., and Altamira, I. (2014). The seven-year enrichment: macrofaunal succession in deep-sea sediments around a 30-tonne whale fall in the Northeast Pacific. *Mar. Ecol. Prog. Ser.* 515, 133–149. doi: 10.3354/meps10955

Smith, C. R., Glover, A. G., Treude, T., Higgs, N. D., and Amon, D. J. (2015). Whale-fall ecosystems: recent insights into ecology, paleoecology, and evolution. *Annu. Rev. Mar. Sci.* 7, 571–596. doi: 10.1146/annurev-marine-010213-135144

Smith, C. R., Roman, J., and Nation, J. B. (2019). A metapopulation model for whale-fall specialists: The largest whales are essential to prevent species extinctions. *J. Mar. Res.* 77 Suppl, 283–302. doi: 10.1357/002224019828474250

Stoeckle, M. (2006). *Species richness of deep-sea wood-boring clams (subfamily Xylophagainae) from the northeast Pacific* (British Columbia, Canada: University of Victoria), 188.

Stramska, M. (2014). Particulate organic carbon in the surface waters of the North Atlantic: spatial and temporal variability based on satellite ocean color. *Int. J. Remote Sens.* 35, 4717–4738. doi: 10.1080/01431161.2014.919686

Sturbois, A., De Cáceres, M., Sánchez-Pinillos, M., Schaal, G., Gauthier, O., Le Mao, P., et al. (2021). Extending community trajectory analysis: New metrics and representation. *Ecol. Model.* 440, 109400. doi: 10.1016/j.ecolmodel.2020.109400

Sumida, P. Y. G., Alfaro-Lucas, J. M., Shimabukuro, M., Kitazato, H., Perez, J. A. A., Soares-Gomes, A., et al. (2016). Deep-sea whale fall fauna from the Atlantic resembles that of the Pacific Ocean. *Sci. Rep.* 6, 22139. doi: 10.1038/srep22139

Thomsen, L., Aguzzi, J., Costa, C., De Leo, F. C., Ogston, A., and Purser, A. (2017). The oceanic biological pump: rapid carbon transfer to depth at continental margins during winter. *Sci. Rep.* 7, 10763. doi: 10.1038/s41598-017-11075-6

Thomsen, L., Barnes, C., Best, M., Chapman, R., Pirenne, B., Thomson, R., et al. (2012). Ocean circulation promotes methane release from gas hydrate outcrops at the NEPTUNE Canada Barkley Canyon node. *Geophysical Res. Lett.* 39, L16605. doi: 10.1029/2012GL052462

Turner, R. D. (1973). Wood-boring bivalves, opportunistic species in the deep sea. *Science* 180, 1377–1379. doi: 10.1126/science.180.4093.1377

Turner, R. D. (1977). Wood, mollusks, and deep-sea food chains. *Bull. Am. Malacological Union* 1976, 13–19.

Turner, R. D. (2002). On the subfamily xylophagainae (Family pholadidae, bivalvia, mollusca). *Bull. Museum Comp. Zoology* 157, 223–307.

Ulanova, N. G. (2000). The effects of windthrow on forests at different spatial scales: a review. *For. Ecol. Manage.* 135, 155–167. doi: 10.1016/S0378-1127(00)00307-8

van den Brink, P. J., and ter Braak, C. J. F. (1999). Principal response curves: Analysis of time-dependent multivariate responses of biological community to stress. *Environ. Toxicol. Chem.* 18, 138–148. doi: 10.1002/etc.5620180207

Vaquer-Sunyer, R., and Duarte, C. (2008). Thresholds of hypoxia for marine biodiversity. *Proc. Natl. Acad. Sci.* 105, 15452–15457. doi: 10.1073/pnas.0803833105

Voight, J. R. (2007). Experimental deep-sea deployments reveal diverse Northeast Pacific wood-boring bivalves of Xylophagainae (Myoida: Pholadidae). *J. Molluscan Stud.* 73, 377–391. doi: 10.1093/mollus/eym034

Voight, J. R. (2008). Deep-sea wood-boring bivalves of *Xylophaga* (Myoida: Pholadidae) on the Continental Shelf: a new species described. *J. Mar. Biol. Assoc. United Kingdom* 88, 1459–1464. doi: 10.1017/S0025315408002117

Voight, J. R. (2009). Diversity and reproduction of near-shore vs offshore wood-boring bivalves (Pholadidae: Xylophagainae) of the deep eastern Pacific ocean, with three new species. *J. Molluscan Stud.* 75, 167–174. doi: 10.1093/mollus/eyp012

Whittaker, T., and Robinson, M. (1923). The calculus of observations, a treatise on numerical mathematics. *Q. J. R. Meteorolog. Soc.* 50, 163–164. doi: 10.1002/qj.49705021024

Wohl, E., and Iskin, E. P. (2021). Damming the wood falls. *Sci. Adv.* 7, eabj0988. doi: 10.1126/sciadv.abj0988

Wolff, T. (1979). Macrofaunal utilization of plant-remains in the deep sea. *Sarsia* 64, 117–136. doi: 10.1080/00364827.1979.10411373

Young, E. L., Halanych, K. M., Amon, D. J., Altamira, I., Voight, J. R., Higgs, N. D., et al. (2022). Depth and substrate type influence community structure and diversity of wood and whale-bone habitats on the deep NE Pacific margin. *Mar. Ecol. Prog. Ser.* 687, 23–42. doi: 10.3354/meps14005

Ziegler, A. F., Smith, C. R., Edwards, K. F., and Vernet, M. (2017). Glacial dropstones: islands enhancing seafloor species richness of benthic megafauna in West Antarctic Peninsula fjords. *Mar. Ecol. Prog. Ser.* 583, 1–14. doi: 10.3354/meps12363